Effects of Non-Plastic Fines Content on Cyclic Resistance and Post Liquefaction of Sand-Silt Mixtures Based on Shear Wave Velocity

F. Askari [*1], R. Dabiri [2], A. Shafiee [1], and M.K. Jafari [3]

1. Assisstant Professor, Geotechnical Engineering Research Center, International Institute of Earthquake Engineering and Seismology (IIEES), Tehran, I.R. Iran
* Corresponding Author; email: askari@iiees.ac.ir
2. PhD of Geotechnical Engineering, Department of Civil Engineering, Islamic Azad University, Tabriz Branch, Tabriz, I.R. Iran
3. Professor, Geotechnical Engineering Research Center, International Institute of Earthquake Engineering and Seismology (IIEES), Tehran, I.R. Iran

ABSTRACT

The cyclic resistance, shear wave velocity and post-liquefaction behavior of saturated Firoozkooh sand with different percentages of non-plastic silt are evaluated. Cyclic triaxial and resonant column tests performed on reconstituted samples prepared in laboratory utilizing undercompaction method. The data obtained from this study along with other existing data were transferred to the field and compared with the field performance curves based on shear wave velocity proposed by Andrus and Stokoe-2000. Then, to observe post-liquefaction behavior of the mixtures, volume change and pore pressure dissipation were measured. Tests results exhibit a clear trend among cyclic resistance, shear wave velocity and post-liquefaction behavior of specimens. In addition, the laboratory results indicated that using the existing field-based correlations may overestimate the cyclic resistance of the Firoozkooh sand-silt mixtures when silt content is 60%. For clean sand and the specimens with up to 30% fines, results of this study are fairly consistent with Andrus and Stokoe correlations. Increasing fines content would increase the final post-liquefaction volumetric strain.

Keywords:
Non-plastic fines;
Cyclic resistance;
Shear wave velocity;
Field performance data;
Cyclic triaxial test

1. Introduction

Field test results such as the *N* value from standard penetration test (*SPT*), cone tip resistance (q_c) from cone penetration test (*CPT*) or shear wave velocity (V_s) have been widely used to assess the liquefaction potential for sand under framework of simplified procedures [1]. The simplified procedure uses an empirical correlation between the cyclic resistance ratios (*CRR*) and the field test results to determine if the soil is potentially liquefiable. Such *CRR* (Cyclic Resistance Ratio) correlation curves have almost been developed for clean sands based on field observations and procedures were suggested to account for sands with fines content. Past experience has shown that mineral contents and plasticity of fines are important contributing factors to monotonic and cyclic behavior of sands that contain fines [2]. Up to now, no clear consensus has been received on influence of non-plastic fines on cyclic resistance of sands. Some researchers concluded that increase of fines increases the liquefaction resistance [3-4], while others indicated that the fines decrease the liquefaction resistance [5]. Also in some studies, it has been found that the sand's resistance to liquefaction will initially decreases as the silt content increases and then increases as the silt content continues to increase [6-7].

Although penetration-based methods (i.e., *SPT* and *CPT*) are well developed [8], penetration tests may be impractical or unreliable at some sites. Meanwhile, shear wave velocity (V_s) offers engineers as a supplementary tool to evaluate liquefaction resistance of soils. Both V_s and liquefaction resistance are similarly but not proportionally influenced by many of the same factors (e.g., void ratio, state stress, stress history, and geologic age). The advantages of a V_s-based method have been discussed by

many researchers [8]. Over the past years, the V_s-based procedure for liquefaction assessment has attracted numerous studies and progressed significantly with improved correlations and more complete data bases. The most prevailing approach nowadays is in-situ V_s measurements at sites shaken by earthquakes [9], which follows the framework of the Seed and Idriss [10] simplified procedure and correlates the overburden stress-corrected shear wave velocity (V_{s1}) to the magnitude-scaled cyclic stress ratio (*CSR*) induced by earthquakes. Most of the measured soil parameters for in-situ V_s testing are post earthquake properties and do not exactly reflect the initial soil states before earthquakes. Thus despite their great practical importance, the field *CRR*-V_{s1} correlations do not furnish insight into the fundamental behavior of liquefiable soils. As it is pointed out by Seed and Idriss [10], with field seismic conditions being properly simulated, the controlled laboratory studies may be used to broaden the applicability of liquefaction criteria, especially for the conditions where little or no field performance data is available. Thereafter many studies have been focusing on this subject on clean sands and sand-silt mixtures [11-20] which demonstrate the validity of laboratory V_s -based methods. The CRR_{field}-V_{s1} correlations developed in the laboratory and have been compared with the field-based correlations [1]. For example, Rouch et al [14].

This paper describes the results of an experimental study on effect of non-plastic fines on the cyclic resistance obtained based on shear wave velocity and post liquefaction (i.e. pore pressure dissipation and volume change) behavior of sands. The data obtained from this study along with other existing data were transferred to the field and compared to the field performance curves proposed by Andrus and Stokoe [8]. Cyclic triaxial and resonant column tests were conducted on reconstituted samples of Firoozkooh sand and sand-silt mixtures prepared in laboratory with various fines contents (*FC* = 15, 30 and 60%) and relative densities (*Dr* = 15, 30, 60 and 75%). Pore pressure dissipations and volume changes of samples were also recorded to observe the post-liquefaction behavior of silty sands. Shear wave velocity of samples were measured by resonant column apparatus and normalized by overburden stresses. Values of cyclic in-situ resistance ratio (CRR_{field}) based on laboratory values versus normalized shear wave velocity (V_{s1}) are developed. Finally, Results of this study and other existing data are compared to field-based correlations purposed by Andrus and Stokoe [8].

2. Experimental Program

The study described herein investigates the effects of non-plastic silt contents on the cyclic resistance based on shear wave velocity and post liquefaction behavior of sands using isotropically-consolidated, undrained cyclic triaxial and resonant column tests. Tests were performed on reconstituted samples prepared in laboratory utilizing undercompaction method. The systems used for conducting tests were automated triaxial testing and fixed-free type, torsional resonant column apparatus. A detailed description of the used soils, sample preparation technique and tests procedure are given below.

2.1. Materials Tested

In this study, the Firoozkooh sand (#.161); a uniformly graded sand (*SP*) with a mean grain size, D_{50}, of 0.25*mm*, coefficient of uniformity, C_u, of 1.75 and a specific gravity of 2.67 was used. The soil grains are sub-angular to sub-round in shape. The non-plastic silt used in tests was derived from the fine-grained portion of the Firoozkooh silty sand. Figure (1) shows the grain size distributions of the soils used in this study. Clean sand with three mixtures of sand-silt was used. The mixtures were obtained by mixing respectively 15, 30, and 60% of silt with sand. The specimens were prepared to achieve after-consolidation relative densities of 15, 30, 60 and 75% depending on their silt content.

The global void ratios (*e*) and the intergrain void

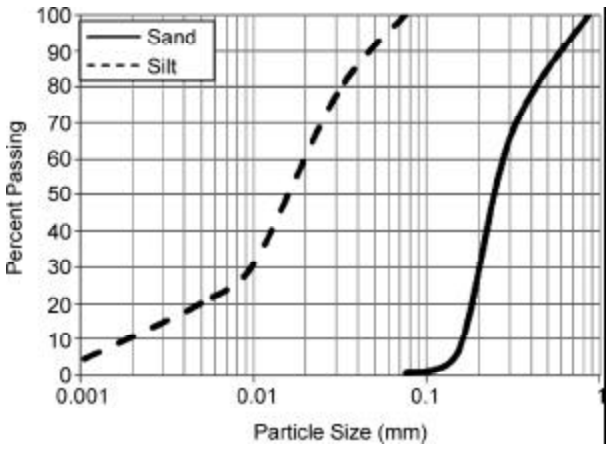

Figure 1. Grain size distribution for soils used in this study.

ratios (e_s = Sand skeleton void ratio is one that exists in a silty sand if all of the silt particle were removed, leaving only the sand grains and voids to form the skeleton) for the mixtures are presented in Table (1). The vibratory table method (*ASTM D*4253) was used to determine the minimum void ratio, e_{min}, meanwhile *ASTTM D*4254 procedure was employed to find the maximum void ratio, e_{max}, see Table (1).

2.2. Sample Preparation

In order to obtain a uniform density throughout the specimens, the undercompaction technique [21] was used. The undercompaction method consists of placing each layer at a density slightly greater than the density of the layer below it in order to account for the decrease in volume and increase in density that occurs in the lower layers when the new layer is placed. In this study, the specimens were made in six layers with an undercompaction value of 5%, so that relative density was varied by 1% per layer. To ensure the uniformity of density throughout the specimens' height, the void ratio distribution within the specimens were obtained. The specimens were solidified and a gelation solution was used [22]. The solidified specimen was then sliced and distribution of void ratio within the test specimen was determined. The measurements revealed that the relative error in achieving the required density throughout the specimens was successfully less than 5% for each layer. For example, the void ratio values of the six layers of sand sample, prepared in 30% relative density was 0.77, 0.76, 0.8, 0.81, 0.8 and 0.81 respectively. In addition, the specimens were prepared in a Plexiglas mold to have better control over the layer's thickness, see Figure (2). During sample preparation, it was found that forming low density specimens for high silt content (i.e. 60%) materials was impossible, because of excessive collapse during saturation. Thus, high silt content specimens were prepared at high relative densities of 60 and 75%, meanwhile other specimens were prepared at densities of 15, 30 and 60%.

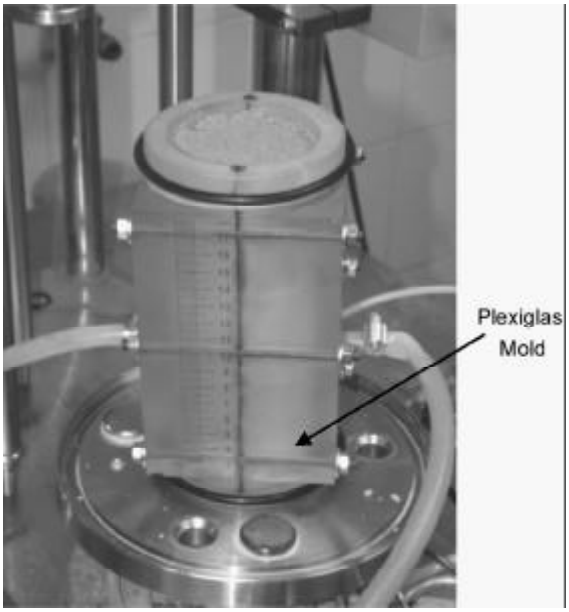

Figure 2. Controlling layer's thickness in plexiglas mold in triaxial apparatus.

2.3. Test Procedure

The *CRR* values were measured using an automated stress-controlled cyclic triaxial apparatus. The specimens were tested with a typical diameter of 70*mm* and a height of 150*mm*. Small strain shear wave velocity, V_s was also measured using a fixed-free type, torsional resonant column apparatus. The tested specimens were typically 70*mm* in diameter and 100*mm* in height. The specimens were saturated with a Skempton B-value in excess of 98%. To facilitate saturation process, carbon dioxide (CO_2) was first percolated through the specimens. Then de-aired water was flushed into the specimens. Finally a back pressure of 100*kPa* was incrementally applied to accelerate saturation rate. Then specimens were isotropically consolidated under an effective confining stress of 100*kPa*. All relative densities reported herein are based on the after-consolidation void ratios. In cyclic triaxial tests, the specimens were loaded sinusoidally at a frequency of 0.1*Hz ASTM D*5311 varying deviator stress at

Table 1. Values of e and e_s for different mixtures.

Type of Materials	e_{min}	e_{max}	Dr = 15%		Dr = 30%		Dr = 60%		Dr = 75%	
			e	e_s	e	e_s	e	e_s	e	e_s
Sand	0.58	0.87	0.83	0.83	0.78	0.78	0.69	0.69	0.65	0.65
Sand+15% Silt	0.41	0.83	0.76	1.08	0.7	1	0.58	0.86	0.51	0.57
Sand+30% Silt	0.32	0.854	0.77	1.52	0.69	1.41	0.53	1.185	0.45	1.07
Sand+60% Silt	0.36	1.259	1.124	-	0.99	-	0.72	-	0.58	-

the appropriate cyclic stress ratio until they were liquefied. In this study, liquefaction was defined and evaluated at initial liquefaction; when the pore pressure in the specimen first equaled the initial confining stress or the specimen reached 5% double amplitude axial strain, whichever occurred first. To observe post liquefaction behavior of the mixtures, once the specimens are liquefied, the cyclic loading phase was terminated and volume change and pore pressure dissipation were measured immediately. Bottom end of each specimen was connected to a volume measuring burette. The top was connected to a pore pressure transducer with no drainage allowed. This setup simulated a one-way drainage condition.

3. Evaluation of Cyclic Resistance and Shear Wave Velocity

Figures (3a), to (3c) presents cyclic stress ratio (*CSR*) expressed versus number of cycles to liquefaction (*N*). Cyclic resistance is defined as the cyclic stress ratio causing initial liquefaction in 15 cycles of loading [23]. *CRR* values and small strain shear wave velocity (V_s), shear modulus (G_{max}) and damping ratio (*D*) of the sand-silt mixtures are presented in Table (2).

As shown in Figures (3a) to (3c) and Table (2), in very loose and medium dense samples (i.e. *Dr* = 15 and 30%), the cyclic resistance of Firoozkooh sand first, slightly increases with fines content up to 15%, followed by a decrease beyond this value. Similar trend was found by Koester [24] through testing on the mixtures of fine sands and non-plastic silts. In dense samples (i.e. *Dr* = 60%), the cyclic resistance continuously decreases with increase in silt contents. The cyclic resistance of the specimens containing 60% silt with *Dr* = 75% are also shown in Figure (3c). As it was expected, cyclic resistance increased with increase in relative density.

The effect of fines on the shear wave velocity have been less studied and understood. Resonant column tests conducted by Iwasaki and Tatsuoka [25] and Huang et al [15] showed that the small strain-shear modulus, G_{max} and therefore V_s decreased with increase in non-plastic fine content. Table (2) shows that, V_s and Maximum shear modulus (G_{max}) in clean sand and sand-silt mixtures increase with increase of relative density. On the other hand, V_s and G_{max} decrease with increase of silt content. On the other hand, in constant relative density, with increasing of fines content up to 30%, G_{max} decreases and then increases with fines content more than 30%.

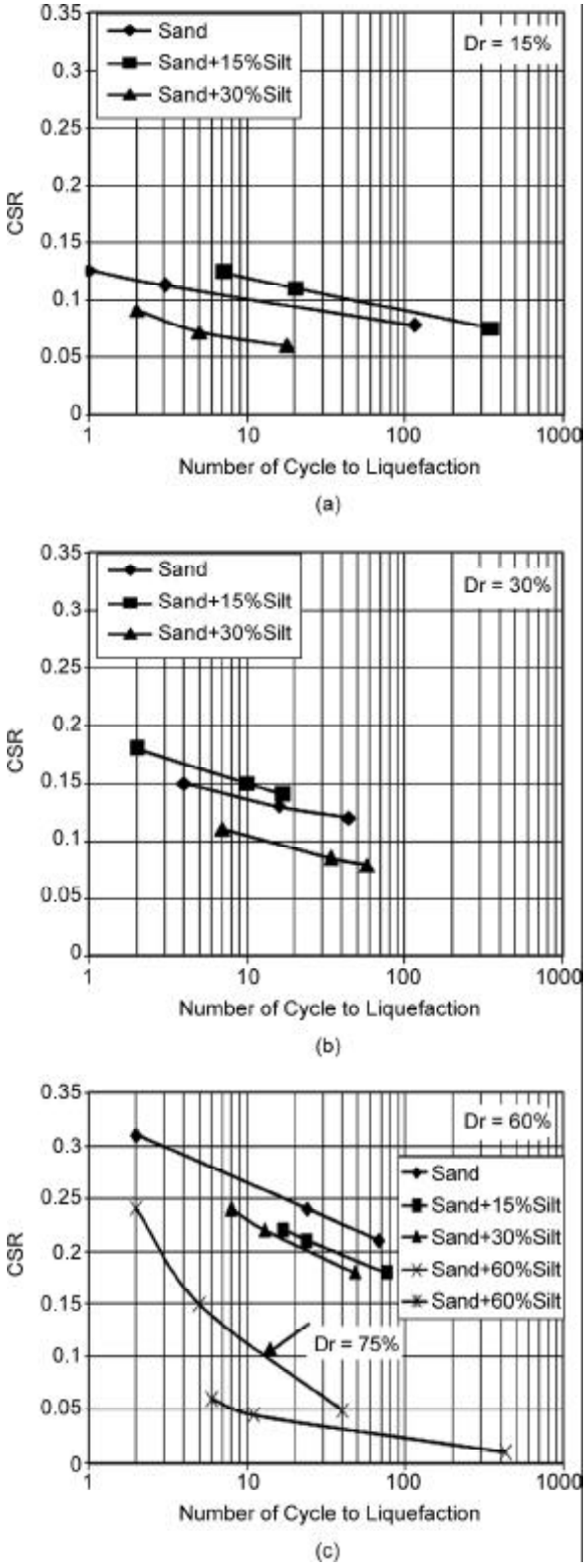

Figure 3. Results of cyclic triaxial tests for the various combinations of sand with silt (a) *Dr* = 15% (b) *Dr* = 30% and (c) *Dr* = 60 and 75%.

Table 2. Results of cyclic triaxial and resonant column tests of sand-silt mixtures.

Type of Material	*Dr*	$CRR_{Triaxial}$	*Vs (m/s)*	G_{max} *(kG/cm²)*	*D(%)*
Sand	0.15	0.096	182	525	4.7
	0.30	0.132	193	742	4.5
	0.60	0.25	201	855	4.3
Sand+15%Silt	0.15	0.112	169	452	4
	0.30	0.142	181	575	3.8
	0.60	0.23	202	744	3.5
Sand+30%Silt	0.15	0.061	157	325	3.8
	0.30	0.096	168	446	3.6
	0.60	0.23	189	691	3.4
Sand+60%Silt	0.60	0.033	164	459	3.6
	0.75	0.093	175	573	3.7

Also damping ratio (*D*) decreases with increasing relative densities. In constant relative density, damping ratio decreases with fines content up to 30%, and then it increases a little with fines content up to 60%. Figures (4a) to (4d) present the variations of *CRR*, V_s, G_{max} and *D* versus sand skeleton void ratio, which can be seen that:

Cyclic resistance ratio increases with sand skeleton void ratio for mixtures having up to 15% silt and decreases with further increase of the silt content. In dense specimens (i.e. $Dr = 60\%$) *CRR* continually decreases with sand skeleton void ratio. Shear wave velocity, maximum shear modulus and damping ratio continuously decrease with sand skeleton void ratio and silt content.

As it is shown in Figure (5), with increasing relative densities from 15% to 75%, V_s value increases. Also, in constant relative density, with increasing of the fines content, shear wave velocity decreases.

4. Conversion of Laboratory Data to Field

It is of great importance to point out, however, that both of the liquefaction resistance (*CRR*) and shear wave velocity (V_s) were obtained in undrained cyclic triaxial and resonant column tests under isotropic consolidation conditions, which are usually different from the in-situ conditions required to be evaluated for design purposes. Therefore, some considerations should be included in applying the laboratory test-based *CRR*-V_s correlations to in-situ conditions. It is common to correct *CRR* to in-situ *CRR* (i.e. CRR_{field}) in an approximate manner as follows [26]:

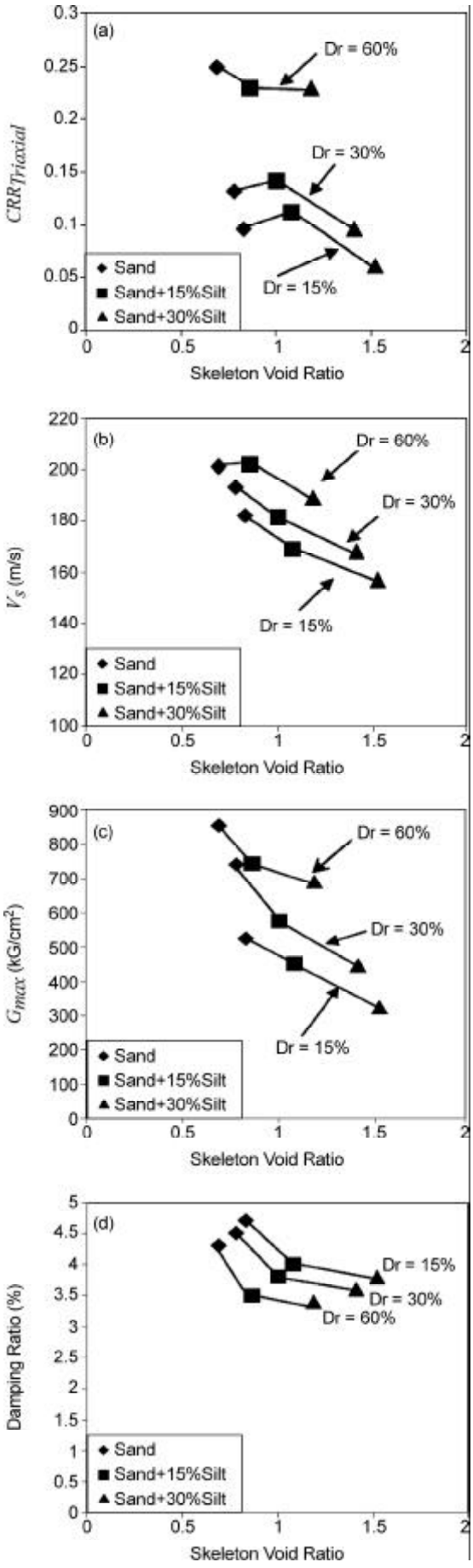

Figure 4. (a) to (d) variation of CRR triaxial, V_s, G_{max} and *D* versus skeleton void ratio.

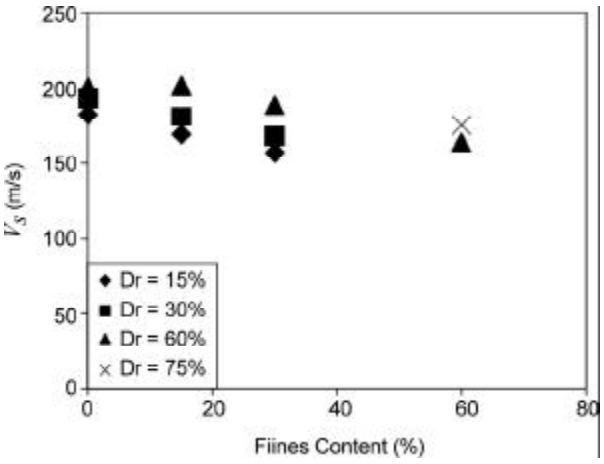

Figure 5. Variation effects of fines content on shear wave velocity.

$$CRR_{field} = \alpha.\beta.CRR_{triaxial} \quad (1)$$

where α and β are correction factors. Some equations presented for α are as follows:

$$\alpha = K_0 \quad (2)$$

$$\alpha = \frac{1+2K_0}{3} \quad (3)$$

$$\alpha = \frac{1+K_0}{2} \quad (4)$$

$$\alpha = \frac{2(1+2K_0)}{3\sqrt{3}} \quad (5)$$

In which K_0 is the effective earth pressure ratio at rest. Eqs. (2) and (3) were proposed by Seed and Peacock [26] and Eqs. (4) and (5) by Finn et al [27] and Castro [28] respectively. K_0 was also taken equal to $(1-\sin\varphi')$, where φ' is angle of shearing resistance. For each mixture at desired relative density, φ' was determined using monotonic undrained triaxial tests conducted under initial confining stresses of 100, 200 and 300*kPa*, see Table (3). Finally, by averaging over the α values from Eqs. (2) to (5), the desired value of constant α was determined, i.e. α_{mean} in Table (3).

β is function of relative density [29] and is defined as:

$$\begin{aligned} &Dr \le 45\% \Rightarrow \beta = 1.15 \\ &Dr \succ 45\% \Rightarrow \beta = 0.01Dr + 0.7 \end{aligned} \quad (6)$$

Table (3) presents the value of β along with CRR_{field} for different mixtures.

On the other hand, the measured V_s require adjustment for different stress states. As V_s was widely observed to depend equally on principal stresses in the direction of wave propagation and particle motion [30], V_s can be expressed as:

$$V_{sf} = V_s\left[\frac{(1+2K_0)}{3}\right]^{0.25} \quad (7)$$

Where V_{sf} = the equivalent field value of laboratory measured V_s. According to common practice [4, 5] the V_{sf} in Eq. (7) should be further corrected in terms of the in-situ effective overburden stress (σ'_V) as follows:

$$V_{s1} = V_{sf}\left(\frac{P_a}{\sigma'_V}\right)^{0.25} = V_s\left(\frac{1+2K_0}{3}\right)^{0.25}\left(\frac{P_a}{\sigma'_m}\right)^{0.25} \quad (8)$$

where V_{s1}= overburden stress-corrected velocity; P_a= atmosphere pressure; and σ'_m = mean effective stress in the laboratory. Table (3) presents the value of V_{s1} for each mixture.

In Table (3), it is seen that values of CRR_{Field} increases as the silt content increases up to 15%. With further increase in silt content up to 30%, cyclic resistance ratio decreases in lower relative

Table 3. CRR_{Field} and V_{s1} for different sand-silt mixtures.

Type of Material	*Dr*	j '(°)	$CRR_{triaxial}$	*Vs (m/s)*	a_{mean}	b	CRR_{field}	Vs_1 *(m/s)*
Clean Sand	0.15	20	0.096	182	0.788	1.15	0.087	170.6
	0.30	29	0.132	193	0.68	1.15	0.103	174.8
	0.60	34	0.25	201	0.63	1.3	0.201	178
Sand+15%Silt	0.15	17	0.112	169	0.83	1.15	0.106	160
	0.30	23	0.142	181	0.752	1.15	0.123	167
	0.60	32	0.23	202	0.65	1.3	0.194	181
Sand+30%Silt	0.15	16.2	0.061	157	0.832	1.15	0.058	149
	0.30	19	0.096	168	0.796	1.15	0.088	157
	0.60	29	0.23	189	0.68	1.3	0.203	171
Sand+60%Silt	0.60	28	0.033	164	0.69	1.3	0.03	149
	0.75	31	0.093	175	0.66	1.45	0.088	157

densities (*Dr* = 15%, 30%). As the silt content increases up to 60%, the CRR_{Field} decreases in dense relative density (*Dr* = 60%) and with the increase of relative density from 60% up to 75%, the CRR_{Field} is increased.

Figure (6) presents the values of CRR_{Field} for different mixtures versus relative densities. It is seen that values of CRR_{Field} increases as the silt content increases up to 15%, with further increase in silt content up to 30%, cyclic resistance ratio decreases in lower relative densities (*Dr* = 15%, 30%). As the silt content increases up to 60%, the CRR is decreased in dense relative density (*Dr* = 60%) and with increase of relative density from 60% up to 75%, the *CRR* is increased.

As can be seen in Figure (7), in lower relative densities (i.e. *Dr* = 15, 30%), the values of steady state friction angle (φ') decreases as the silt content increase up to 30%. With increasing silt content to 60%, φ' values slightly increase.

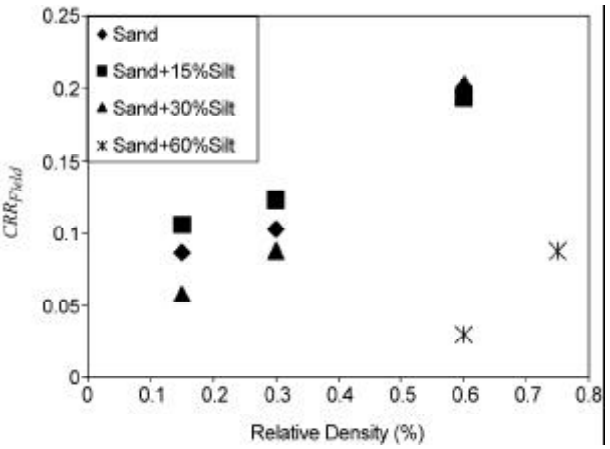

Figure 6. Effects of nonplastic fine content on cyclic resistance ratio (*CRR*) vs. relative densities.

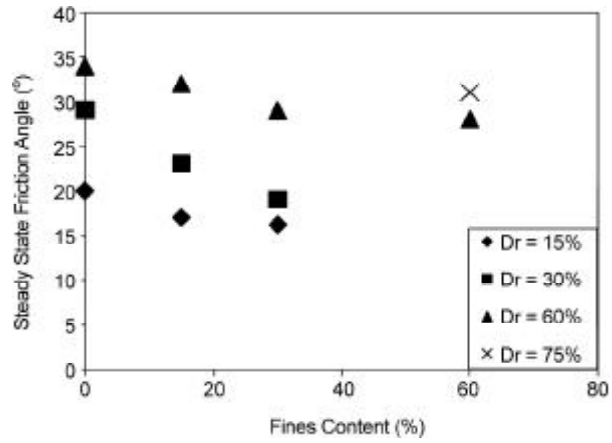

Figure 7. Variations effects of fines content on steady state friction angle.

5. Comparison of Converted Laboratory Results with Field-Based Correlations

The CRR_{field}-V_{s1} correlations developed from the laboratory results of this study and other studies are compared to the field-based correlations of Andrus and Stokoe [17] for different ranges of fines content (*FC*) as:

1) The laboratory-based correlations for clean sands ($FC \leq 5\%$) that are based on the data from this study, Tokimatsu et al [31]; Rouch et al [14]; Huang et al [15]; Liu et al [18], see Figure (8);
2) The laboratory-based correlations for silty sands with $5\% \prec FC \prec 30\%$ that are based on the data from this study, Rouch et al [14]; Huang et al [15] Liu et al [18], see Figure (9); and
3) The laboratory-based correlations for sand-silt mixtures ($FC \geq 35\%$) that are based on the data from this study, Huang et al [14] and Baxter et al [20], see Figure (10).

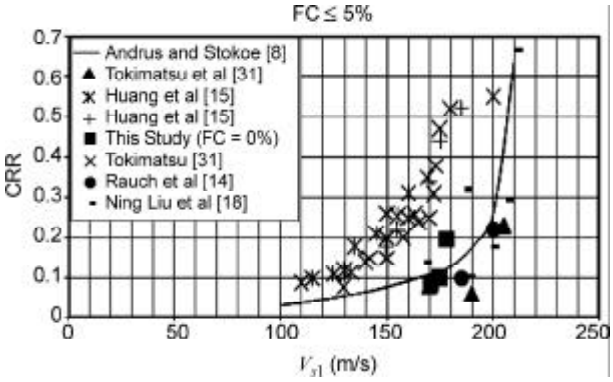

Figure 8. Comparison between converted CRR_{field}-V_{s1} data based on the laboratory data from san-silt mixtures ($FC \leq 5\%$) and the existing field-based correlation of Andrus and Stokoe [8].

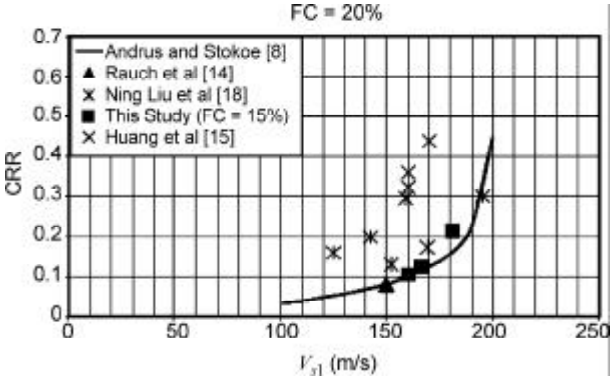

Figure 9. Comparison between converted CRR_{field}-V_{s1} data based on the laboratory data from san-silt mixtures ($5\% \prec FC \prec 30\%$) and the existing field-based correlation of Andrus and Stokoe [8].

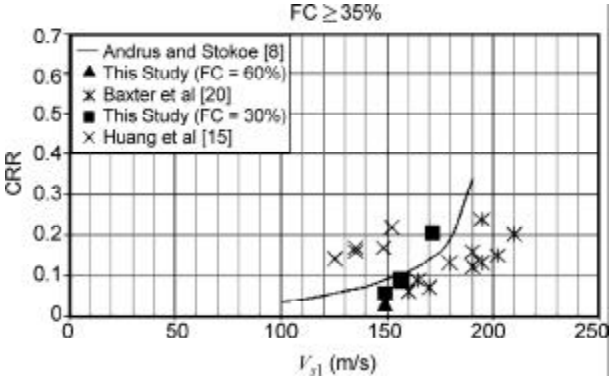

Figure 10. Comparison between converted CRR_{field}-V_{s1} data based on the laboratory data from san-silt mixtures ($FC \geq 30\%$) and the existing field-based correlation of Andrus and Stokoe [8].

Figure (8) shows the CRR_{field} - V_{s1} correlation for the clean sand used in this study. As can be seen, converted CRR_{field} - V_{s1} data based on the laboratory data from clean sand is located in the right side of the semi-empirical curve proposed in the simplified procedure for fines content of less than 5%. Similarly, the trends in the laboratory data on sands with 15% fines content shown in Figure (10), is found to be consistent with the liquefaction curve developed by Andrus and Stokoe [8] for $FC = 20\%$ from field performance data. As it is shown in Figure (11), the laboratory-based correlations from this study for FC = 30 and 60% plot below the field-based curve for $FC > 30\%$. Therefore, although the results are not sufficient in order to judge well, but based on the results of this study, using the field-based correlation would overestimate the liquefaction resistance of these sand-silt mixtures.

Differences may be due to techniques used for sample preparation in the laboratory which significantly affects the measured cyclic resistance and shear wave velocity, the cyclic stress path generated by uniform cycles of axial stress in a triaxial test which only approximately models an earthquake loading on a soil deposit, the uncertainty of the relationships between the laboratory and field conditions accounted for the correction of cyclic triaxial strength ($CRR_{triaxial}$) to in-situ cyclic resistance ratios (CRR_{field}), and the assessment of cyclic strength and shear wave velocity in separate soil specimens. On the other hand, the doubt in field performance data may originate from the uncertainties in the plasticity of the fines in the in-situ soils, using post earthquake properties that do not exactly reflect the initial soil states before earthquakes and the assumption that CRR_{field} is equal to the CSR obtained from Seed and Idriss [10] well known equation.

6. Post-Liquefaction Response of Sand-Silt Mixtures

When saturated loose sand deposits are subjected to shaking during an earthquake, pore water pressure is known to build up leading to liquefaction or loss of strength. The pore water pressure then starts to dissipate mainly towards the ground surface, accompanied by some volume change of the sand deposits which is manifested on the ground surface as settlement. The volume change characteristics of sand due to dissipation of pore water pressures induced by undrained cyclic loading has been studied in the laboratory tests by Lee and Albaisa [32], and Tatsuoka et al [33]. As a result of these studies, it has become apparent that the volumetric strain after liquefaction is influenced not only by the density but more importantly by the maximum shear strain which the sand has undergone during the application of cyclic loads. On the basis of this rationale, an attempt was made by Tokimatsu and Seed [34] to deploy a methodology to predict the post liquefaction settlement of ground. An alternative procedure for estimating ground settlement was explored by Ishihara and Yoshimine [35] by maximum shear strain which is a key parameter influencing the post liquefaction volumetric strain.

This procedure is based on results of extensive laboratory tests. Detailed understanding of post-liquefaction behavior of the sand-silt mixtures, including pore pressure dissipation and densification characteristics can give insight to the behavior of the silty sand. It can also be used for evaluation of post-liquefaction settlement and design of drainage systems to mitigate liquefaction. At present, there is only limited data available on this subject and data is primarily limited to clean sands. Thevanayagam and Martin [36] recently studied the post liquefaction of silty sands. To observe post-liquefaction behavior of the mixtures, once specimen liquefied, the cyclic loading phase was terminated and volume change and pore pressure dissipation were measured immediately. Volume change was measured from the bottom end of the specimen, whilst pore pressure dissipation was measured from the top end of the specimen. Figure (11) shows the variation of dissipated post-liquefaction pore pressure versus

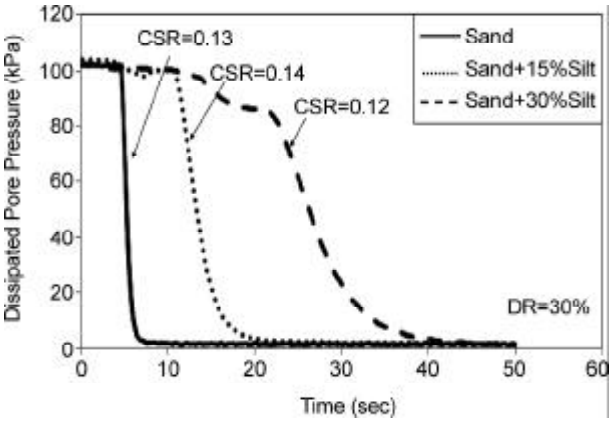

Figure 11. Variation of dissipated pore pressure vs. time in specimens of sand-silt mixtures, σ'_o = 100kPa.

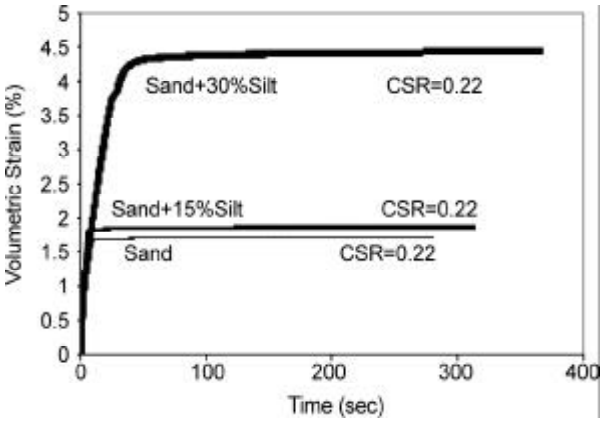

Figure 13. Variation of volumetric strain vs. time in specimens of sand-silt mixtures (Dr = 60%), σ'_o = 100kPa.

time for $\sigma' = 100kPa$ and relative density of 30% (*CSR* about 0.13).

As it can be seen, when silt content is raised, the required time for dissipation of the generated pore pressure is also increased. For example, specimen containing 30% fines require more time to dissipate all the generated pore pressure with respect to specimen without silt content (other specimens have the same behavior). The observed trend is logical, since void ratio and subsequently permeability decrease when silt content is raised.

Figure (12) shows variations of volumetric strain versus relative densities for all of specimens. An interesting feature of post-liquefaction behavior which can be found is that higher final volumetric strain would be attained when silt content is raised. This means that increasing silt content causes a looser fabric to be formed.

Figure (13) shows the post-liquefaction densification for sand-silt mixtures in $\sigma'_o = 100kPa$ and relative density of 60% (*CSR* about 0.21). The figure presents variation of the volumetric strain (i.e. volume of water expelled out of the specimen divided by the end of consolidation volume of specimen) versus time for sand-silt mixtures. Also, the figure shows that volumetric strain increases with time, reaching to a constant value (i.e. final volumetric strain). However, for specimens containing fines content, because of lower permeability, the time needed to reach the final volumetric strain is more (other specimens have the same behavior). Generally, it can be seen that in all the specimens, as the silt content increase up to 30%, the final volumetric strain increases.

Diagrams in Figures (11) to (13) show that increasing silt content causes a looser fabric to be formed and in this regard, sand skeleton void ratio may describe this behavior better.

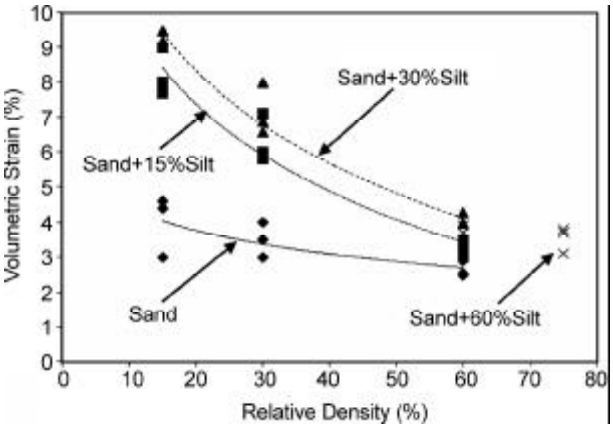

Figure 12. Variation of volumetric strain vs. relative density in specimens of sand-silt mixtures, σ'_o = 100kPa.

7. Conclusion

The results of an experimental study on the liquefaction behavior of reconstituted specimens of non-plastic sand-silt mixtures at different fines content and relative densities based on shear wave velocity were presented. Cyclic resistance, shear wave velocity and post-liquefaction behavior of the mixtures were studied. The results of this study along with other studies were compared to field based *CRR*-V_{s1} curves prepared by Andrus and Stokoe [8]. The following conclusions regarding the effects of non-plastic fines on the liquefaction susceptibility of sands can be drawn from this study:

- When the soil is loose or medium dense (i.e. *Dr* = 15 and 30%), the *CRR* of Firoozkooh sand

increases slightly with fines content up to 15%, followed by a decrease beyond this value. In dense samples (i.e. *Dr* = 60%), the cyclic resistance ratio of Firoozkooh sand continuously decreases with increase of silt content.

- Data obtained on the cyclic resistance, shear wave velocity and dynamic properties of the mixtures evidently show that, *CRR*, V_s, G_{max} and Damping ratio have good correlation with skeleton void ratios. It can be generally concluded that increase in fines content leads to decrease in cyclic strength, shear wave velocity, maximum shear modulus and damping ratios.
- In conversion of laboratory data to field condition, results show that the CRR_{field}-V_{s1} correlation for the clean sand lie closely to the semi-empirical curve proposed in the simplified procedure for fines content less than 5% by Andrus and Stokoe [8]. This trend is also observed in the converted laboratory data of this study on sands with 15% fines content and results are consist with the liquefaction boundary curves developed by Andrus and Stokoe [8] for $FC = 20\%$. The CRR_{field}-V_{s1} values for $FC = 30$ and 60% in present research are below the field-based curve for $FC \geq 35\%$, means that field-based correlation overestimates the liquefaction resistance of these sand-silt mixtures in comparison with the present study.
- When silt content is raised to 30% and more, the required time for dissipation of the post-liquefaction pore pressure is increased. Furthermore, increase of fines content to 30% and more leads to more final volumetric strains without any dependence on maximum shear strains.
- In general, when fines content is raised to 30% and more, the stability of the mixture fabric seems to be reduced. Data obtained from cyclic resistance, shear wave velocity, maximum shear modulus and damping ratio of mixtures evidently show that, increasing of fines content to 30% and more lead to less *CRR*, V_s, G_{max} and *D*.

Acknowledgements

This research was conducted in the International Institute of Earthquake Engineering and Seismology (*IIEES*) and supported under the Contract No. 6712, which is gratefully appreciated.

References

1. Youd, T.L., Idriss, I.M., Andrus, R.D., Arango, R.C., Castro, G., Christian, J.T., Dobry, R., Finn, W.D.L., Harder, Jr., L.F., Hynes, M.E., Ishihara, K., Koester, J.P., Liao, S.S.C., Marcuson, III, W.F., Martin, G.R., Mitchell, J.K., Moriwaki, Y., Power, M.S., Robertson, P.K., Seed, R.B., and Stokoe, II, K.H. (2001). "Liquefaction Resistance of Soils: Summary Report from the 1996 NCEER and 1998 NCEER/NSF Workshop on Evaluation of Liquefaction Resistance of Soils", *Journal of Geotechnical and Geoenvironmental Engineering, ASCE*, **127**(10), 817-833.

2. Ishihara K. (1993). "Liquefaction and Flow Failure during Earthquake", *Geotechnique*, **43**(3), 351-415.

3. Seed, H.B., Idriss, I.M., and Arango, I. (1983). "Evaluation of Liquefaction Potential Using Field Performance Data", *J. of Geotechnical Engineering*, **109**(3), 458-482.

4. Amini, F. and Qi, G.Z. (2000). "Liquefaction Testing of Stratified Silty Sands", *Journal of Geotechnical and Geoenviromental Engineering, ASCE*, 208-217.

5. Lade, P.V. and Yamamuro, J.A. (1997). "Effects of Nonplastic Fines on Static Liquefaction of Sands", *Canadian Geotechnical Journal*, **34**(6), 918-928.

6. Polito, C.P. and Martin, J.R. (2001). "Effects of Non Plastic Fines on the Liquefaction Resistance of Sands", *Journal of Geotechnical and Geoenviromental Engineering, ASCE*, **127**(5), 408-415.

7. Xenaki, V.C. and Athanasopoulos, G.A. (2003). "Liquefaction Resistance of Sand-Silt Mixtures: An Experimental Investigation of the Effect of Fines", *Journal of Soil Dynamic and Earthquake Engineering*, **23**(3), 183-194.

8. Andrus, R.D. and Stokoe II, K.H. (2000). "Liquefaction Resistance of Soils from Shear Wave Velocity", *Journal of Geotechnical and Geoenvironmental Engineering, ASCE*, **126**(11), 1015-1025.

9. Andrus, R.D., Stokoe II., K.H., and Juang, C.H.

(2004). "Guide for Shear Wave-Based Liquefaction Potential Evaluation", *Earthquake Spectra*, **20**(2), 285-308.

10. Seed, H.B. and Idriss I.M. (1971). "Simplified Procedure for Evaluating Soil Liquefaction Potential", *Journal of Soil Mechanics and Foundation Division, ASCE*, **97**(9), 1249-1273.

11. Kayen, R., Seed, R.B., Moss, R.E., Cetin, K.O., Tanaka, Y., and Tokimatsu, K. (2004). "Global Shear Wave Velocity Database for Probabilistic Assessment of the Initiation of Seismic-Soil Liquefaction", *11th International Conference on Soil Dynamics and Earthquake Engineering*, Berkeley.

12. Dobry, R., Stokoe, K.H., Ladd, R.S., and Youd, T.L. (1981). "Liquefaction Susceptibility from S-Wave Velocity", *Proc. In-Situ Tests to Evaluate Liquefaction Susceptibility, ASCE National Convention,* St Louis, MO.

13. Tokimatsu, K. and Uchida, A. (1990). "Correlation between Liquefaction Resistance and Shear Wave Velocity", *Journal of Soils and Foundation*, **30**(2), 33-42.

14. Rouch, A.F., Duffy, M., and Stokoe, K. (2000). "Laboratory Correlation of Liquefaction Resistance with Shear Wave Velocity", *Journal of Geotechnical and Geoenviromental Engineering, Geotechnical Special Publication, ASCE*, **101**(3), 66-80.

15. Huang, Y.T., Huang, A.B., Chen, K.Y., and Dou, T.M. (2004). "A Laboratory Study on the Undrained Strength of a Silty Sand from Central Western Taiwan", *Journal of Soil Dynamics and Earthquake Engineering*, **24**(9-10), 733-743.

16. Chen, Y.M., Ke, H., and Chen, R.P. (2005). "Correlation of Shear Wave Velocity with Liquefaction Resistance Based on Laboratory Tests", *Journal of Soil Dynamics and Earthquake Engineering*, **25**(6), 461-469.

17. Zhou, Y.G. and Chen, Y.M. (2005). "Influence of Seismic Cyclic Loading History on Small Strain Shear Modulus of Saturated Sands", *Journal of Soil Dynamics and Earthquake Engineering*, **25**(5), 341-353.

18. Ning Liu, S.M., Mitchell, J.K., and Hon, M. (2006). "Influence of Non plastic Fines on Shear Wave Velocity-Based Assessment of Liquefaction", *J. of Geotechnical and Geoenviromental Engineering, ASCE*, **132**(8), 1091-1097.

19. Zhou, Y.G. and Chen, Y.M. (2007). "Laboratory Investigation on Assessing Liquefaction Resistance of Sandy Soils by Shear Wave Velocity", *Journal of Geotechnical and Geoenviromental Engineering, ASCE*, **133**(8), 959-927.

20. Baxter, C.D.P., Bradshaw, A.S., Green, R.A., and Wang, J. (2008). "Correlation Between Cyclic Resistance and Shear Wave Velocity for Providence Silts", *Journal of Geotechnical and Geoenviromental Engineering, ASCE*, **134**(1), 37-46.

21. Ladd, R.S. (1978). "Preparing Test Specimens Using under Compaction", Printed by American Society for Testing and Material, 16-23.

22. Emery, J.J., Finn, W.D.L., and Lee, K.W. (1973). "Uniformity of Saturated Sand Samples", ASTM Special Publishing, 182-194.

23. Ishihara, K. (1996). "Soil Behavior in Earthquake Geotechnics", Oxford Univ. Press, Newyork.

24. Koester, J.P. (1993). "Effects of Fines Type and Content on Liquefaction Potential of Low-to Medium Plasticity Fine-Grained Soils", *National Earthquake Conference, Earthquake Hazard Reduction in the Central and Eastern United States, A Time for Examination and Action*, 67-75.

25. Iwasaki, T. and Tatsuoka, F. (1977). "Effects of Grain Size and Grading on Dynamic Shear Moduli of Sands", *Soils and Foundations*, **17**(3), 9-35.

26. Seed, H.B. and Peacock, W.H. (1971). "The Procedure for Measuring Soil Liquefaction Characteristics", *Journal of the Soil Mechanics and Foundation Division, ASCE*, **97**(SM8), 1099-1119.

27. Finn, W.D.L., Pickering, D.J., and Bransby, P.L. (1971). "Sand Liquefaction in Triaxial and Simple Shear Tests", *Journal of the Soil Mechanics and Foundation Division, ASCE*, **97**(SM4),

639-659.

28. Castro, G. (1976). "Liquefaction and Cyclic Mobility of Saturated Sands", *Journal of Geotechnical Engineering Division, ASCE*, **101**(GT6), 551-569.

29. Das, B.M. (1992). "Principles of Soil Dynamics", Pws-Kent Publishing Company, USA.

30. Belloti, R., Jamiolkowski, J., LoPresti, D.C.F., and O'Niell, D.A. (1996). "Anisotropy of Small Srain Stiffness in Ticino Sand", *Geotechnique*, **46**(1), 115-131.

31. Tokimatsu, K., Yamazuka, T., and Yoshimi, Y. (1986). "Soil Liquefaction Evaluations by Elastic Shear Moduli", *J. of Soils and Foundation*, **26**(1), 25-35.

32. Lee, K.L. and Albaisa, A. (1974). "Earthquake Settlements in Saturated Sands", *Journal of Geotechnical Engineering Division, ASCE*, **100**(4), 387-406.

33. Tatsuoka, F., Sasaki, T., and Yamada, S. (1984). "Settlement in Saturated Sand Induced by Cyclic Undrained Simple Shear", *Proc. of 8th World Conf. on Earthquake Engineering*, San Francisco, (3), 255-262.

34. Tokimatsu, K. and Seed, H.B. (1987). "Evaluation of Settlements in Sands due to Earthquake Shaking", *Journal of Geotechnical Engineering Division, ASCE*, **113**(8), 861-878.

35. Ishihara, K. and Yoshimine, M. (1992). "Evaluation of Settlements in Sand Deposits Following Liquefaction during Earthquake", *Journal of Soils and Foundations*, **32**(1) ,173-188.

36. Thevanayagam, S. and Martin, G.R. (2003). "Liquefaction and Post-Liquefaction Dissipation/ Densification Characteristics of Silty Soils", MCEER Highway Project, Task E2-1, Annual Report: Research Year 1.